100-mJ, 100-W Cryogenically Cooled Yb:YLF Laser

Mikhail Pergament,[1*] Martin Kellert,[1] Umit Demirbas,[1,4] Jelto Thesinga,[1] Simon Reuter,[1] Yizhou Liu,[1,2] Yi Hua,[1,2] Muharrem Kilinc,[1] Alexey Yakovlev[1] and Franz X. Kärtner[1,2,3]

[1]*Center for Free-Electron Laser Science CFEL, Deutsches Elektronen-Synchrotron DESY, Notkestr. 85, 22607 Hamburg, Germany*
[2]*Physics Department, University of Hamburg, Luruper Chaussee 149, 22761 Hamburg, Germany*
[3]*The Hamburg Centre for Ultrafast Imaging, Luruper Chaussee 149, 22761 Hamburg, Germany*
[4]*Department of Electrical and Electronics Engineering, Antalya Bilim University, 07190 Dosemealti, Antalya, Turkey*
**Corresponding author: mikhail.pergament@desy.de*

Received XX Month XXXX; revised XX Month, XXXX; accepted XX Month XXXX; posted XX Month XXXX (Doc. ID XXXXX); published XX Month XXXX

We present a diode-pumped Yb:YLF laser system generating 100-mJ sub-ps pulses at a 1 kHz repetition rate (100 W average power) by chirped-pulse amplification. The laser consists of cryogenically-cooled 78K, regenerative, and 8-pass booster amplifier seeded by an all-fiber front end. The output pulses are compressed to 980 fs in a single grating Treacy compressor with a throughput of 89%. The laser will be applied to multi-cycle THz generation and pumping of high-average power parametric amplifiers. © 2023 Optica Publishing Group

Numerous scientific and technological applications demand high-energy and high-average power lasers as enabling tool. Especially optical parametric chirped-pulse amplifiers (OPCPA) providing sub-femtosecond pulses [1,2], THz generation [3,4], spectral broadening followed by pulse compression [5–7] and high harmonic generation (HHG) [8] enormously benefit from a reliable laser source with output pulse durations below 1 ps. All these applications request very similar laser parameters to enable high efficiency and performance: pulse durations shorter than 1 ps., and good beam quality. However, pulse energy requirements could vary from tens to hundreds of millijoules at kilohertz repetition rates. As a result, the average power could reach challenging kilowatt levels, which makes a thermoptical design of the lasers crucial. The classical engineering response is the increase of the gain medium cooling surface–volume ratio, employ of Yb^{3+} as an active laser dopant due to its low quantum defect and availability of industrial-grade high-brilliance laser diodes. The result is ytterbium-based room-temperature laser technologies such as thin-disk, Innoslab, and coherently combined fiber systems. The thin-disk and Innoslab approach are to change the geometry of the gain medium to increase the cooling surface while reducing the overall volume. Although this makes it possible to achieve an average power of kW and an output of hundreds of millijoules, it requests highly-engineered multi-pass construction of the laser pump and laser pulse propagation design [9,10]. Unfortunately, further steps to increase output energy and average power may eventually bring those technologies to their limits and excessively complicates the laser design. In coherently combined fiber laser systems where the heat is distributed along the fiber, non-linear effects limit the stretched pulse energy to ~100s microjoules per large mode area fiber and currently, 12 large-core fibers have now been coherently combined to increase power to 10.4 kW at 80 MHz [11]. So far, the maximum energy achieved with this technology is 10 mJ [12]. Although coherent fiber combining technology has reached an average output power level of ten kilowatts, the next step in increasing the output pulse energy beyond tens of millijoules requires further comprehensive development with significant challenges in fiber combining and production [13].

Operating ytterbium lasers at cryogenic temperatures further improves the thermo-optical strength of the host and increases emission cross section and gain at the expense of reduced gain bandwidth[14–16]. That allows reaching comparable output parameters with significantly simplified laser geometries. Unfortunately, the best effort in Yb:YAG high-energy cryogenic amplifiers has an output pulse duration of around 5 ps due to strong spectral narrowing at cryogenic temperatures. Despite a more than 8-fold drop in thermo-optic effect, due to the positive thermo-optic coefficient of Yb:YAG, the realization of more than 50 W of average output power in rod-type geometries at cryogenic temperatures is difficult. This leads to introducing of more advanced Yb:YAG amplification elements with composite discs, complicating the overall amplifier structure [17,18]. One possible step for further development of cryogenic ytterbium lasers is to find another host crystal with more acceptable laser characteristics. Recent research shows different gain material, Yb:YLF, with more than 10 nm gain bandwidth and a negative thermo-optic effect at cryogenic temperatures, making it an attractive alternative to reach sub-picosecond pulses at high average output power levels [19,20]. Yb:YLF is a uniaxial crystal, that exhibits the different spectral and thermoptical properties for E//a and E//c axes, opening up exciting

new horizons for cryogenic laser development. The previous efforts developing cryogenic cooled Yb: YLF amplifiers demonstrate a high average power regenerative amplifier reaching 250W with a maximum of 20 mJ pulse energy or a low repetition rate (10 Hz) multi-pass amplifier outputted 300 mJ [21,22]. Here, we aim at a multi-stage amplifier laser system applicable as a reliable kilohertz laser source for THz generation and OPCPA pumping. We illustrate the schematic of the 100 W average power cryogenic Yb:YLF laser system in Fig.1. The full-fiber front end is composed of an Yb-doped femtosecond fiber oscillator, employing an all-normal-dispersion (ANDi) mode-locking [23] and followed by the nonlinear parabolic pulse amplifier after the Gaussian spectral filter. The output is stretched by chirped fiber Bragg gratings (CFBG). The stretcher constructed of two gratings, the first CFBG has a chirp rate of 306 ps/nm and the second one 100 ps/nm, while the latter of them has tuning capability. These CFBGs are designed to compensate for the dispersion of a 1760 lines/mm grating Treacy compressor operated at a 60-deg incidence angle, and have 7.5 nm reflection bandwidth centered at 1019nm.

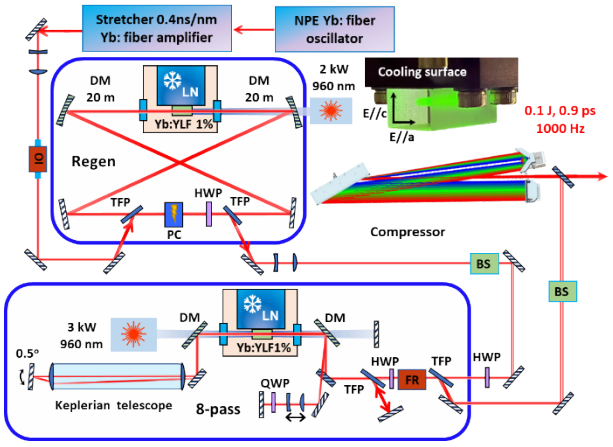

Fig. 1. Schematic of the 100 mJ cryogenic Yb:YLF laser system. Regen, regenerative amplifier; TFP, thin-film-polarizer; FR, Faraday rotator; HWP, half-wave plate; OI, optical isolator; LN, liquid Nitrogen Dewar; PC, Pockels cell; BS, beam- stabilization unit; QWP, quarter-wave plate. Inset: The crystal geometry

The front-end provides 20 nJ pulses with 2.5 nm full-width-half-maximum (FWHM) centered at 1018 nm stretched to 1 ns imaged to 2.2 mm beam size into the bow-tie regenerative amplifier through the Faraday isolator. The pulse enters the amplifier cavity by reflecting from the TFP and is picked by a water-cooled BBO Pockels cell (rise/fall time 3.5ns/8ns) and a half-wave plate. The 3 m long cavity consists of two dichroic concave mirrors (DM) and two flat mirrors with high reflectance (HR), this arrangement ensures stability of the resonator for a wide range of thermal lensing under high pumping conditions at different repetition rates. We employ a 2 cm long 1% Yb:YLF rod crystal with an aperture of 10 mm x 15 mm with two 3 mm undoped caps adhesive-free bonded on both optical faces. The caps reduce surface deformation under strong end-pumping. The crystal is metal soldered from the top to the tungsten-copper heat-spreader and thermally connected through the compressed metal gasket to cooling plate of the Dewar (Fig.1 inset). Using an a-cut Yb:YLF-crystal allows us to exploit both E//a and E//c axes for amplification, depending on the selected polarization. The Dewar is cooled to 78K by boiling liquid Nitrogen. A 2 kW, 960 nm industrial fiber-coupled diode module pumps the crystal with a gated 250 µs pump pulse duration with an absorption efficiency of 95%. The driving current of the laser diode is optimized to 220 watts of absorbed power, corresponding to 20 mJ output energy at 1 kHz repetition rate. The p-polarized pulse travels through the cavity exposed to E//a gain of the Yb:YLF crystal, which helps to keep almost the seeder's initial bandwidth. The PC switches the pulse from the cavity by the reflection on the second TFP after 80 round trips. The beam is magnified in a Galilean telescope to 3.6 mm diameter and directed to an 8-pass amplifier, and due to pristine (M^2=1.1) beam quality, no relay imaging is necessary. The output energy stability corresponds to 5 % RMS, and the active beam stabilization system controls beam pointing. The measurement was performed at an output energy of 20 mJ over 6 hours.

The p-polarized beam enters the 8-pass amplifier through the Faraday rotator, a pair of TFPs, and HWP. Then, after a couple of reflections on the z-fold mirror pair, it goes through the second 1% Yb-doped YLF crystal with similar specs, installed into the identical Dewar cooled by liquid nitrogen. The vacuum Keplerian 2-f telescope images the beam from the center of the crystal to the back-reflecting mirror, which returns the beam to the system with a slight (0.5 deg) angular detuning. The beam returns to the crystal center bypassing the input mirror and is transferred to the alternative path with the compensation Galilean telescope (f =-75 cm and f = 100cm), which counteracts the thermal lens in the Yb:YLF crystal. After double passing the telescope and the quarter-wave plate (QWP), the beam retroreflects back to the system. We use the compensation telescope not only to counteract the thermal lens in the cavity but to gradually increase the beam size through the propagation up to 3.9 mm to avoid high fluences close to the damage threshold. Then completing four passes, the s-polarized beam returns to the entrance of the amplifier but reflects back from the TFP to return to the system for an additional four passes. Finally, the amplified beam leaves the system due to the action of a Faraday rotator and TFP. The crystal is pumped by a 3kW industrial laser diode unit, with a pumping pulse duration of 250 µs.

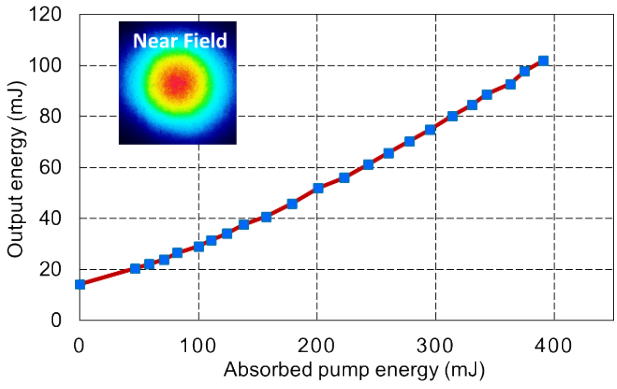

Fig. 2. Measured variation of output laser pulse energy as a function of absorbed pump energy at 1 kHz. Inset: Near field beam profile at 102 mJ.

The driving current is tuned to reach 390 W absorbed power with an absorption efficiency of 95 % when the pump beam is double-passed. The dependence of output pulse energy on absorbed pump pulse energy is shown in Fig. 2.

We extract 102 mJ from the 8-pass amplifier, corresponding to 20% of optical to-optical efficiency. The near-field beam profile shows a 97% Gaussian intensity distribution in Fig. 2 (inset). The M^2 measurement exhibits 1.21 in horizontal and 1.12 in vertical direction (Fig. 3). Given that the output beam of the regenerative amplifier has an M^2 of 1.1, we can explain the apparent decline of the beam quality coefficient in the horizontal direction by the horizontal angular detuning in the Kepler 2-f telescope. The small off-axis propagation caused the spherical aberration and deteriorated the beam quality. The beam intensity distribution in the planes along the M^2 scan remains Gaussian (insets) Fig.3. We believe that the main reason for the obtained good beam quality at such high pulse energies and high average power levels is the negative thermo-optic effect (dn/dT) of Yb:YLF. The Yb:YLF crystal at cryogenic temperatures has a negative dn/dT of -0.5×10^{-6} K^{-1} and -1.8×10^{-6} K^{-1} at E//a and E//c, respectively, which helps to balance other thermal lensing effects such as mechanical stress and bulging.

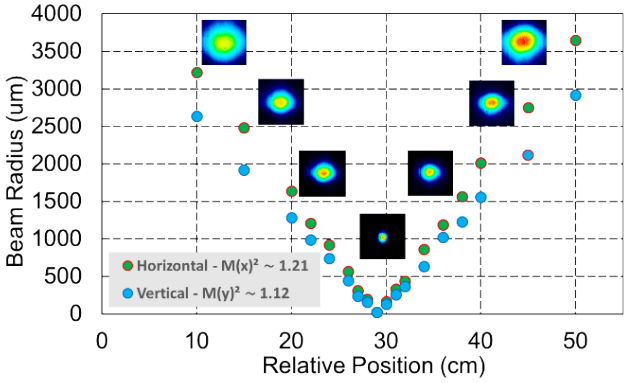

Fig. 3. M^2 measurement of beam quality of the compressed 100 mJ pulse. The insets show the beam profiles at different caustic positions.

The polarization multiplexing sequence of the 8-pass amplifier is as follows: the first two passes of the laser pulse with E//a gain through the Yb:YLF crystal and E//c gain in the subsequent four passes, the last two passes are completed with E//a gain. Peak emission cross sections (ECS) of Yb:YLF E//a (0.75×10^{-20} cm^2) and E//c (2.4×10^{-20} cm^2) at cryogenic temperature are spectrally shifted to each other. This not only maintains the output spectrum of the regenerative amplifier, but also extends it somewhat into the longer wavelength region (Fig. 4). A more than 3-fold difference in gain between the E//c and E//a passes results in a significant imbalance in energy extraction, but the approximately 20 mJ extracted during E//a amplification has a visual impact on the final compressed pulse duration. At the same time, we want to point out that using both gain axes helps us to simultaneously benefit from good E//c energy extraction and broadband E//a gain. The order of polarization multiplexing can be changed by including an additional HWP after the TFP. We note an interesting lack of dependence of the energy and spectrum of the amplified pulse on the order of polarization multiplexing. The spectral bandwidth of the output pulse is only 2 nm FWHM, which is the result of the limited and not optimally distributed bandwidth of the seed source.

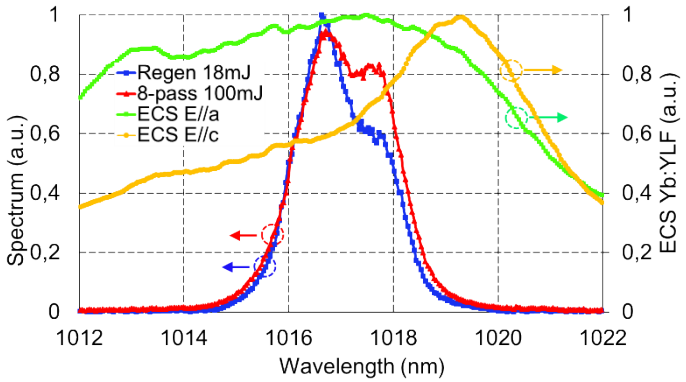

Fig. 4. Measured optical spectra at the output of the regenerative amplifier (blue), and the output of the final amplifier (red). Normalized emission cross section of Yb:YLF for E//a (green) and E//c (yellow) axes at 78 K.

The amplified laser pulse is compressed in a single grating Treacy compressor, with a high-efficiency multi-layer dielectric grating (1760 lines/mm) at 60° angle of incidence with a throughput of 89%. We choose the single grating layout due to its ease of alignment and tuning. The HR coated return 90° retro-reflector and roof-mirror are installed with 10 µrad precision. The 980 fs FWHM pulse duration was measured by second-harmonic autocorrelation with the $sech^2$ fit, presented on Fig.5. We attribute the 15% pedestal to the unfortunate fact that we use CFBG at a slightly offset wavelength where the group delay lacks apodization. Hence, we assign the pedestal to higher-order dispersion, which cannot be compensated by compressor or stretcher tuning.

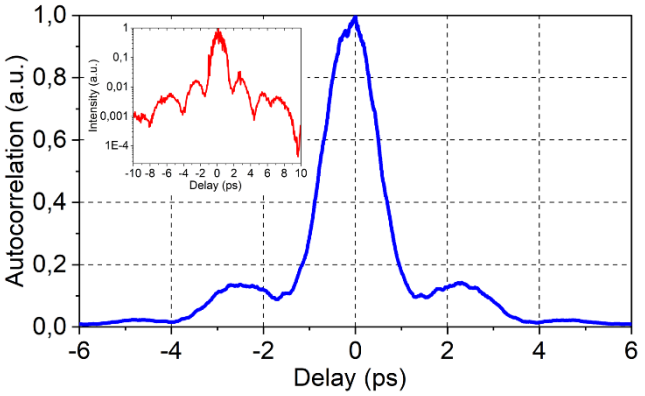

Fig. 5. Compressed pulse duration measured by second-harmonic autocorrelation. The $sech^2$ fit corresponds to a pulse duration of 0.98 ps FWHM. Inset: Measured third order autocorrelation.

The measured third-order autocorrelation (Fig.5 inset) reveals high symmetry and confirms the overall good dispersion compensation up to the third order.

In conclusion, we have demonstrated a chirped pulse amplification laser system based on cryogenically cooled Yb:YLF rod-type

amplifiers. The system delivers more than 100 mJ of laser pulses with pristine beam quality at a repetition rate of 1 kHz. We have compressed the output pulse to 980 fs in the Treacy compressor. The laser system is planned to be used as a pumping source for THz generation, OPCPA pumping, and multi-pass cell pulse compression experiments, where the level of technology is approaching pulse energies above 100 mJ [24]. The results achieved give confidence in the significant scalability potential of cryogenic Yb:YLF laser technology. However, there are two main factors limiting the system development. Firstly, the observed threshold for laser induced damage under vacuum cryogenic conditions is about 3 J/cm^2 for a 1 ns pulse, which limits the extraction of the amplifier at low repetition rates. The second issue is the rod geometry which can only effectively absorb 600 W of average pump power, reaching its cooling capacity limit. As a solution, we are currently preparing a new seeder source for the system, providing 10 nm spectral bandwidth, centered at 1016 nm. This seed pulse at the same 0.4 ns/nm chirp rate will have a duration of about 4 ns and allow for high fluences and more efficient extraction. In addition, this bandwidth is necessary to utilize the full Yb:YLF gain and can lead to compressed output pulse duration of about 300 fs. Detailed thermal simulation shows that changing the crystal geometry to a slab will extend the pump's absorbed power limit to 1 kW average power. Overall, we hope to achieve at least a 3-fold increase in output energy and average power in future studies.

Funding. Seventh Framework Program (FP7) FP7/2007-2013 European Research Council (ERC) Synergy Grant (609920).

Acknowledgments. The authors acknowledge support from previous group members L. E. Zapata, K. Zapata for establishing the indium-bonding technology for YLF at CFEL-DESY. We also acknowledge the contributions of Thomas Tilp, Andrej Berg, and Andre Hoemke.

Disclosures. The authors declare no conflicts of interest.

References

1. G. Andriukaitis, H. C. Kapteyn, A. Pugžlys, M. M. Murnane, S. Ališauskas, T. Balčiūnas, M.-C. Chen, T. Popmintchev, and A. Baltuška, Opt. Lett. Vol. 36, Issue 15, pp. 2755-2757 **36**, 2755 (2011).
2. G. M. Rossi, R. E. Mainz, Y. Yang, F. Scheiba, M. A. Silva-Toledo, S. H. Chia, P. D. Keathley, S. Fang, O. D. Mücke, C. Manzoni, G. Cerullo, G. Cirmi, and F. X. Kärtner, Nat. Photonics **14**, 629 (2020).
3. F. X. Kärtner, F. Ahr, A. L. Calendron, H. Çankaya, S. Carbajo, G. Chang, G. Cirmi, K. Dörner, U. Dorda, A. Fallahi, A. Hartin, M. Hemmer, R. Hobbs, Y. Hua, W. R. Huang, R. Letrun, N. Matlis, V. Mazalova, O. D. Mücke, E. Nanni, W. Putnam, K. Ravi, F. Reichert, I. Sarrou, X. Wu, A. Yahaghi, H. Ye, L. Zapata, D. Zhang, C. Zhou, R. J. D. Miller, K. K. Berggren, H. Graafsma, A. Meents, R. W. Assmann, H. N. Chapman, and P. Fromme, Nucl. Instrum. Methods Phys. Res. A. **829**, 24 (2016).
4. G. Polónyi, B. Monoszlai, G. Gäumann, E. J. Rohwer, G. Andriukaitis, T. Balciunas, A. Pugzlys, A. Baltuska, T. Feurer, J. Hebling, J. A. Fülöp, T. Kampfrath, K. Tanaka, K. A. Nelson, R. Huang, K. Hong, K. Ravi, A. Fallahi, G. Moriena, R. J. D Miller, F. X. Kärtner, H. Hirori, A. Doi, and F. Blanchard, Opt. Express, Vol. 24, Issue 21, pp. 23872-23882 **24**, 23872 (2016).
5. A. L. Viotti, S. Alisauskas, A. Bin Wahid, P. Balla, N. Schirmel, B. Manschwetus, I. Hartl, and C. M. Heyl, J. Synchrotron Radiat. **28**, 36 (2021).
6. S. Gröbmeyer, K. Fritsch, B. Schneider, M. Poetzlberger, V. Pervak, J. Brons, and O. Pronin, Appl. Phys. B Lasers Opt. **126**, (2020).
7. Y. Pfaff, C. Forster, G. Barbiero, M. Rampp, S. Klingebiel, J. Brons, C. Y. Teisset, H. Wang, R. Jung, J. Jaksic, A. H. Woldegeorgis, C. J. Saraceno, and T. Metzger, Opt. Express, Vol. 30, Issue 7, pp. 10981-10990 **30**, 10981 (2022).
8. T. Popmintchev, M. C. Chen, D. Popmintchev, P. Arpin, S. Brown, S. Ališauskas, G. Andriukaitis, T. Balčiunas, O. D. Mücke, A. Pugzlys, A. Baltuška, B. Shim, S. E. Schrauth, A. Gaeta, C. Hernández-García, L. Plaja, A. Becker, A. Jaron-Becker, M. M. Murnane, and H. C. Kapteyn, Science (80-.). **336**, 1287 (2012).
9. C. Wandt, C. Herkommer, D. Bauer, K. Michel, P. Krötz, P. Walch, R. Kienberger, R. Bessing, R. Jung, S. Klingebiel, T. Metzger, T. Produit, and T. Metzger, Opt. Express, Vol. 28, Issue 20, pp. 30164-30173 **28**, 30164 (2020).
10. P. Russbueldt, T. Mans, J. Weitenberg, H. D. Hoffmann, and R. Poprawe, Opt. Lett. **35**, 4169 (2010).
11. M. Müller, C. Aleshire, A. Klenke, E. Haddad, F. Légaré, A. Tünnermann, and J. Limpert, Opt. Lett. **45**, 3083 (2020).
12. H. Stark, J. Buldt, M. Müller, A. Klenke, and J. Limpert, Opt. Lett. **46**, 120 (2021).
13. A. Steinkopff, C. Aleshire, A. Klenke, C. Jauregui, and J. Limpert, Opt. Express, Vol. 30, Issue 10, pp. 16896-16908 **30**, 16896 (2022).
14. T. Y. Fan, D. J. Ripin, R. L. Aggarwal, J. R. Ochoa, B. Chann, M. Tilleman, and J. Spitzberg, IEEE J. Sel. Top. Quantum Electron. **13**, 448 (2007).
15. U. Demirbas, M. Kellert, J. Thesinga, Y. Hua, S. Reuter, F. X. Kärtner, and M. Pergament, Appl. Phys. B **127**, 46 (2021).
16. J. Kawanaka, M. Fujita, and K. Yamakawa, Artic. Laser Phys. **15**, 1306 (2005).
17. Y. Wang, H. Chi, C. Baumgarten, K. Dehne, A. R. Meadows, A. Davenport, G. Murray, B. A. Reagan, C. S. Menoni, and J. J. Rocca, Opt. Lett. **45**, 6615 (2020).
18. L. E. Zapata, M. Pergament, M. Schust, S. Reuter, J. Thesinga, C. Zapata, M. Kellert, U. Demirbas, A.-L. Calendron, Y. Liu, and F. X. Kärtner, Opt. Lett. Vol. 47, Issue 24, pp. 6385-6388 **47**, 6385 (2022).
19. L. E. Zapata, T. Y. Fan, D. J. Ripin, V. Chvykov, V. Chvykov, H. Chi, Y. Wang, K. Dehne, M. Berrill, J. J. Rocca, J. J. Rocca, and J. J. Rocca, Opt. Lett. Vol. 35, Issue 11, pp. 1854-1856 **35**, 1854 (2010).
20. U. Demirbas, M. Kellert, J. Thesinga, S. Reuter, F. X. Kärtner, and M. Pergament, Opt. Mater. Express, Vol. 12, Issue 7, pp. 2508-2528 **12**, 2508 (2022).
21. U. Demirbas, M. Kellert, J. Thesinga, Y. Hua, S. Reuter, M. Pergament, and F. X. Kärtner, Opt. Lett. Vol. 46, Issue 16, pp. 3865-3868 **46**, 3865 (2021).
22. Y. Liu, U. Demirbas, M. Kellert, J. Thesinga, H. Cankaya, Y. Hua, L. E. Zapata, M. Pergament, and F. X. Kärtner, OSA Contin. Vol. 3, Issue 10, pp. 2722-2729 **3**, 2722 (2020).
23. W. H. Renninger and F. W. Wise, in *2013 Conference on Lasers and Electro-Optics Europe and International Quantum Electronics Conference, CLEO/Europe-IQEC 2013* (IEEE Computer Society, 2013).
24. A.-L. Viotti, M. Seidel, E. Escoto, S. Rajhans, W. P. Leemans, I. Hartl, and C. M. Heyl, Opt. Vol. 9, Issue 2, pp. 197-216 **9**, 197 (2022).

Publication list with titles

1. G. Andriukaitis, H. C. Kapteyn, A. Pugžlys, M. M. Murnane, S. Ališauskas, T. Balčiūnas, M.-C. Chen, T. Popmintchev, and A. Baltuška, "90 GW peak power few-cycle mid-infrared pulses from an optical parametric amplifier," Opt. Lett. Vol. 36, Issue 15, pp. 2755-2757 **36**(15), 2755–2757 (2011).
2. G. M. Rossi, R. E. Mainz, Y. Yang, F. Scheiba, M. A. Silva-Toledo, S. H. Chia, P. D. Keathley, S. Fang, O. D. Mücke, C. Manzoni, G. Cerullo, G. Cirmi, and F. X. Kärtner, "Sub-cycle millijoule-level parametric waveform synthesizer for attosecond science," Nat. Photonics **14**(10), 629–635 (2020).
3. F. X. Kärtner, F. Ahr, A. L. Calendron, H. Çankaya, S. Carbajo, G. Chang, G. Cirmi, K. Dörner, U. Dorda, A. Fallahi, A. Hartin, M. Hemmer, R. Hobbs, Y. Hua, W. R. Huang, R. Letrun, N. Matlis, V. Mazalova, O. D. Mücke, E. Nanni, W. Putnam, K. Ravi, F. Reichert, I. Sarrou, X. Wu, A. Yahaghi, H. Ye, L. Zapata, D. Zhang, C. Zhou, R. J. D. Miller, K. K. Berggren, H. Graafsma, A. Meents, R. W. Assmann, H. N. Chapman, and P. Fromme, "AXSIS: Exploring the frontiers in attosecond X-ray science, imaging and spectroscopy," Nucl. Instrum. Methods Phys. Res. A. **829**, 24–29 (2016).
4. G. Polónyi, B. Monoszlai, G. Gäumann, E. J. Rohwer, G. Andriukaitis, T. Balciunas, A. Pugzlys, A. Baltuska, T. Feurer, J. Hebling, J. A. Fülöp, T. Kampfrath, K. Tanaka, K. A. Nelson, R. Huang, K. Hong, K. Ravi, A. Fallahi, G. Moriena, R. J. D Miller, F. X. Kärtner, H. Hirori, A. Doi, and F. Blanchard, "High-energy terahertz pulses from semiconductors pumped beyond the three-photon absorption edge," Opt. Express, Vol. 24, Issue 21, pp. 23872-23882 **24**(21), 23872–23882 (2016).
5. A. L. Viotti, S. Alisauskas, A. Bin Wahid, P. Balla, N. Schirmel, B. Manschwetus, I. Hartl, and C. M. Heyl, "60 fs, 1030 nm FEL pump-probe laser based on a multi-pass post-compressed Yb:YAG source," J. Synchrotron Radiat. **28**, 36–43 (2021).
6. S. Gröbmeyer, K. Fritsch, B. Schneider, M. Poetzlberger, V. Pervak, J. Brons, and O. Pronin, "Self-compression at 1 µm wavelength in all-bulk multi-pass geometry," Appl. Phys. B Lasers Opt. **126**(10), (2020).
7. Y. Pfaff, C. Forster, G. Barbiero, M. Rampp, S. Klingebiel, J. Brons, C. Y. Teisset, H. Wang, R. Jung, J. Jaksic, A. H. Woldegeorgis, C. J. Saraceno, and T. Metzger, "Nonlinear pulse compression of a thin-disk amplifier and contrast enhancement via nonlinear ellipse rotation," Opt. Express, Vol. 30, Issue 7, pp. 10981-10990 **30**(7), 10981–10990 (2022).
8. T. Popmintchev, M. C. Chen, D. Popmintchev, P. Arpin, S. Brown, S. Ališauskas, G. Andriukaitis, T. Balčiunas, O. D. Mücke, A. Pugzlys, A. Baltuška, B. Shim, S. E. Schrauth, A. Gaeta, C. Hernández-García, L. Plaja, A. Becker, A. Jaron-Becker, M. M. Murnane, and H. C. Kapteyn, "Bright coherent ultrahigh harmonics in the kev x-ray regime from mid-infrared femtosecond lasers," Science (80-.). **336**(6086), 1287–1291 (2012).
9. C. Wandt, C. Herkommer, D. Bauer, K. Michel, P. Krötz, P. Walch, R. Kienberger, R. Bessing, R. Jung, S. Klingebiel, T. Metzger, T. Produit, and T. Metzger, "Ultrafast thin-disk multipass amplifier with 720 mJ operating at kilohertz repetition rate for applications in atmospheric research," Opt. Express, Vol. 28, Issue 20, pp. 30164-30173 **28**(20), 30164–30173 (2020).
10. P. Russbueldt, T. Mans, J. Weitenberg, H. D. Hoffmann, and R. Poprawe, "Compact diode-pumped 1.1 kW Yb:YAG Innoslab femtosecond amplifier," Opt. Lett. **35**(24), 4169 (2010).
11. M. Müller, C. Aleshire, A. Klenke, E. Haddad, F. Légaré, A. Tünnermann, and J. Limpert, "10.4 kW coherently combined ultrafast fiber laser," Opt. Lett. **45**(11), 3083 (2020).
12. H. Stark, J. Buldt, M. Müller, A. Klenke, and J. Limpert, "1 kW, 10 mJ, 120 fs coherently combined fiber CPA laser system," Opt. Lett. **46**(5), 120 (2021).
13. A. Steinkopff, C. Aleshire, A. Klenke, C. Jauregui, and J. Limpert, "Mitigation of thermally-induced performance limitations in coherently-combined multicore fiber amplifiers," Opt. Express, Vol. 30, Issue 10, pp. 16896-16908 **30**(10), 16896–16908 (2022).
14. T. Y. Fan, D. J. Ripin, R. L. Aggarwal, J. R. Ochoa, B. Chann, M. Tilleman, and J. Spitzberg, "Cryogenic Yb3+-doped solid-state lasers," IEEE J. Sel. Top. Quantum Electron. **13**(3), 448–458 (2007).
15. U. Demirbas, M. Kellert, J. Thesinga, Y. Hua, S. Reuter, F. X. Kärtner, and M. Pergament, "Comparative investigation of lasing and amplification performance in cryogenic Yb:YLF systems," Appl. Phys. B **127**(3), 46 (2021).
16. J. Kawanaka, M. Fujita, and K. Yamakawa, "Dramatically improved laser characteristics of diode-pumped Yb-doped materials at low temperature," Artic. Laser Phys. **15**(9), 1306–1312 (2005).
17. Y. Wang, H. Chi, C. Baumgarten, K. Dehne, A. R. Meadows, A. Davenport, G. Murray, B. A. Reagan, C. S. Menoni, and J. J. Rocca, "1.1 J Yb:YAG picosecond laser at 1 kHz repetition rate," Opt. Lett. **45**(24), 6615 (2020).
18. L. E. Zapata, M. Pergament, M. Schust, S. Reuter, J. Thesinga, C. Zapata, M. Kellert, U. Demirbas, A.-L. Calendron, Y. Liu, and F. X. Kärtner, "One-joule 500-Hz cryogenic Yb:YAG laser driver of composite thin-disk design," Opt. Lett. Vol. 47, Issue 24, pp. 6385-6388 **47**(24), 6385–6388 (2022).
19. L. E. Zapata, T. Y. Fan, D. J. Ripin, V. Chvykov, V. Chvykov, H. Chi, Y. Wang, K. Dehne, M. Berrill, J. J. Rocca, J. J. Rocca, and J. J. Rocca, "Power scaling of cryogenic Yb:$LiYF_4$ lasers," Opt. Lett. Vol. 35, Issue 11, pp. 1854-1856 **35**(11), 1854–1856 (2010).
20. U. Demirbas, M. Kellert, J. Thesinga, S. Reuter, F. X. Kärtner, and M. Pergament, "Advantages of YLF host over YAG in power scaling at cryogenic temperatures: direct comparison of Yb-doped systems," Opt. Mater. Express, Vol. 12, Issue 7, pp. 2508-2528 **12**(7), 2508–2528 (2022).
21. U. Demirbas, M. Kellert, J. Thesinga, Y. Hua, S. Reuter, M. Pergament, and F. X. Kärtner, "Highly efficient cryogenic Yb:YLF regenerative amplifier with 250 W average power," Opt. Lett. Vol. 46, Issue 16, pp. 3865-3868 **46**(16), 3865–3868 (2021).
22. Y. Liu, U. Demirbas, M. Kellert, J. Thesinga, H. Cankaya, Y. Hua, L. E. Zapata, M. Pergament, and F. X. Kärtner, "Eight-pass Yb:YLF cryogenic amplifier generating 305-mJ pulses," OSA Contin. Vol. 3, Issue 10, pp. 2722-2729 **3**(10), 2722–2729 (2020).
23. W. H. Renninger and F. W. Wise, "High-performance fiber lasers based on self-similar pulse propagation," in *2013 Conference on Lasers and Electro-Optics Europe and International Quantum Electronics Conference, CLEO/Europe-IQEC 2013* (IEEE Computer Society, 2013).
24. A.-L. Viotti, M. Seidel, E. Escoto, S. Rajhans, W. P. Leemans, I. Hartl, and C. M. Heyl, "Multi-pass cells for post-compression of ultrashort laser pulses," Opt. Vol. 9, Issue 2, pp. 197-216 **9**(2), 197–216 (2022).